Multiobjective Optimization of Heat-Treated Copper Tool Electrode on EMM Process Using Artificial Bee Colony (ABC) Algorithm

Optimization of Machining Parameters on Laser Beam Machining of Titanium Alloy (Ti 3Al-2.5V) Using Taguchi Method

R. Manoj Samson, T. Geethapriyan, S. Senkathir, Ashwin Ashok and Aditya Rajesh

Abstract As titanium alloy (Ti 3Al-2.5V) has high strength and stiffness with excellent corrosion resistance, it finds its application in aerospace and industrial application. Ti grade 9 is hard, and we have adopted CO_2 laser beam techniques to machine Ti grade 9. We have chosen oxygen and nitrogen gases as assisted gases. Of the various laser beam energy techniques, carbon dioxide laser beam is found to be one of the emerging trends in machining complicated and circuitous parts with maximum accuracy and in less time. Design of experiment is represented by Taguchi's L9 orthogonal array. Two sets of experiments were conducted with oxygen and nitrogen as assisted gases. Material removal rate and surface roughness were calculated and optimized using group Taguchi relational analysis. It is found that surface finish and material removal rate are improved by using nitrogen gas for machining titanium alloy (Ti 3Al-2.5V) using CO_2 laser.

Keywords Taguchi method · Titanium alloy · CO_2 laser

1 Introduction

Compared to the conventional type of machining technique, non-conventional type provides us with one of the non-contact-type machining tools to machine hard metal like titanium alloy. In this paper work involves the cutting of titanium alloy grade 9 sheet using CO_2 laser beam. Literature says that laser beam has the potential to machine the surface of hard material up to 3 mm and of various process parameters such as laser power, cutting speed, pressure and density, where laser power and cutting speed produce cut quality surface finish. This laser beam works on the

R. M. Samson (✉) · T. Geethapriyan · S. Senkathir · A. Ashok · A. Rajesh
Department of Mechanical Engineering, SRM University, Kattankulathur, Chennai 603203, India
e-mail: manoj.sam6@gmail.com

K. S. Vijay Sekar et al. (eds.), *Advances in Manufacturing Processes*, Lecture Notes in Mechanical Engineering, https://doi.org/10.1007/978-981-13-1724-8_46

principle of population inversion of electrons, that is majority of the electrons are excited to higher energy unstable state from lower energy stable state due to absorption of energy from the external source. This titanium alloy grade 9 sheet is cut at varying gas pressure, cutting speed, laser power and focal point. Different focal point is obtained using different lenses like plano-convex lens and meniscus lens. Meniscus lens provides sharp small spot with high power density which is a mandatory parameter for cutting hard metal. This lens is generally made from zinc selenide, gallium arsenide and germanium with high transmissivity to provide small spot size with high power density. Plano-convex lens is used in application where relatively large focal length is required. The gas used is fixed either oxygen or nitrogen, keeping this constant other parameters like cutting speed, gas pressure, laser power and focal point are varied and this is done for both the gases. Based on the results, suitable design is suggested material removal rate and surface roughness for both nitrogen and oxygen. After obtaining the optimized material removal rate and surface roughness, verification of the integrity of the results obtained is carried out. This optimization of the machining parameters is done by Grey-Taguchi approach, and it was confirmed by conducting a confirmation test. The graph which was generated using Minitab 17 software clearly represents of each input parameter over the response parameter. Keeping 95% as the confidence limit, error obtained for each of the response parameter for both material removal rate and surface roughness is calculated.

2 Experimental Set-up

2.1 Laser-Cutting System

Metal cutting is performed by using the state-of-the-art CO_2 laser-cutting method. High-power laser Rofin-Sinar CO_2 is used for metal cutting. Schematic diagram for laser-cutting layout is described below.

2.2 Beam Delivery

The most important component in the CO_2 laser beam is the quality of beam it produces, which includes the laser power, work area and the correct time of beam delivery. A beam delivery mechanism comprises of one mirror telescope, beam bending mirrors and a phase changer.

2.3 Lenses

2.3.1 Meniscus Lens

These are the lenses made from high transmissivity ratio especially made from zinc selenide, gallium arsenide and germanium. These types of lenses are used to obtain shot spot size with high power density. Focal length, diameter, shape and coating are all the design variables, which will directly interfere with the working of CO_2 laser. Principle states that the more shorter the focal length, the more laser power it will produce with short focal depth and small focused spot size. These lenses have one-side surface concave and the other-side convex as shown in the Fig. 3.3, and this arrangement creates a lesser beam diameter, thus truncating the spherical abbreviation beam waste.

2.3.2 Plano-Convex Lens

It has one surface convex and the other surface is simply plain; this is the most simplest combination of all possible lenses. These lenses generally find an application, where obtaining a small focal length is not relatively important. The lenses are placed in such a manner that flat surface should face towards the work piece, while the convex surface always faces towards the laser source.

2.4 Nozzle

A nozzle is typically used to increase the flow rate of gases. From theory of gas dynamics, each types of nozzle is unique in properties. In this experiment, a supersonic minimal length nozzle gives the best design for shock-free flow, ease of manufacturing and minimum nozzle length. Supersonic nozzle has a contracting part followed by an expansion part as per the desired gas properties and Mach number [1]. For commercial laser-cutting operation, sonic nozzles are preferred. They are generally not preferred for thin material since assist inlet gas pressure should be higher to get good quality and better surface finish [2].

2.5 Talysurf Coherence Correlation Interferometer (CCI)

Surface roughness of the machined surface of the work piece is measured using non-contact-type "Talysurf CCI LITE". The average roughness value for each sample is measured as shown in Fig. 3.6. It is simply a 3D surface roughness profiler used for measuring microroughness and step height measurement with 1 angstrom resolution. It has a magnification of 5×, 10×, 20×, 25× and 50×.

2.6 Scanning Electron Microscope

This type of microscope focuses electron beam to produce image of the specimen. The interaction of the electron with the atom in the sample produces various electrical signals that brief about sample's surface topology and its composition. The heat-affected zone of the work piece is captured during the analysis, and results are obtained accurately. Magnification obtained is from 30× to 800000×. Image resolution of about 3 nm can be obtained.

2.7 Selection of Materials

Titanium and its alloys showcase a unique combination of mechanical and physical properties. Moreover, corrosion resistance, which have made them desirable for critical applications in aircrafts, industrial influence, chemical and energy industry service [3], shows excellent elevated temperature properties up to 600 °C and high melting point. Titanium alloys are found to exhibit excellent fatigue strength, resistance to fracture, long life, non-toxic, non-allergenic and fully biocompatible. The most important property is its non-magnetic property.

2.8 Selection of Process Parameter

All the input and output parameters are classified into different types under each category as follows.

2.8.1 Variable Parameters for N_2

Keeping N_2 gas, nozzle diameter—1 mm, stand-off distance 0.7 mm, gating frequency—10,000 Hz all these parameters as fixed, the experiment is carried out at three different levels as shown in Table 1. Gas pressure for N_2 is kept to be almost double as compared to O_2 in order to obtain the optimum results, and this is purely done on trial-and-error basis.

2.8.2 Variable Parameters for O_2

Keeping N_2 gas, nozzle diameter—1 mm, stand-off distance 1 mm, gating frequency-10,000 Hz all these parameters as fixed, the experiment is carried out at three different levels as shown in Table 2.

Table 1 Variable parameters for N_2

Factors	Laser power	Gas pressure	Cutting speed	Focal point
Units	W	Bar	m/min	mm
Level 1	3000	8	1900	0
Level 2	3500	9	2000	−1
Level 3	4000	10	2100	1

Table 2 Variable parameters for O_2

Factors	Laser power	Gas pressure	Cutting speed	Focal point
Units	W	Bar	m/min	mm
Level 1	1200	1.0	2.5	0
Level 2	1300	0.6	2.7	−1
Level 3	1400	0.8	2.9	1

2.9 Design of the Experiment (DOE)

DOE is one of the most important tools that could be used in various experimental analyses. It not only allows various input factors to be analysed, determining their corresponding effect on the output, but also helps to identify any missed out important interaction, which would have been overlooked while taking input parameters at the same time [4].

2.10 DOE Procedure

DOE can be performed in multiple ways. One of the most economical approaches, which satisfies the ultimate need of the problem solving and process design optimization project, would be Taguchi approach. The work piece used here is alloy material titanium alloy (Ti 3Al-2.5V) dimensions of the product 400 × 500. In machining, we use two different gasses, oxygen and nitrogen [5]. Two sets of L9 orthogonal array for machining are given in the table for two different gasses. The machining has both constant and variable parameters, according to orthogonal array to find the output parameters of MRR and SR. After the experiment is done, calculate the MRR and find the SR by surface roughness tester. Calculate the *S*/*N* ratio, normalized *S*/*N* ratio and grey-relational grade by the formula. Give the rank to the grey-relational grade and get optimized value from the rank the highest value is optimized value. The input parameter/dependent parameter and output/independent parameter are to be optimized using nine different experiments [6], which are been carried out as shown in the Table 3. This parameter is taken by using oxygen as an inert gas. However, we have four variables and three levels. Table 3 shows the table for oxygen.

Table 3 Table for O_2

Experiment number	Laser power (W)	Gas pressure (bar)	Cutting speed (m/min)	Focal position (mm)
1	1200	1.0	2.5	0
2	1200	0.6	2.7	−1
3	1200	0.8	2.9	1
4	1300	1.0	2.7	1
5	1300	0.6	2.9	0
6	1300	0.8	2.5	−1
7	1400	1.0	2.9	−1
8	1400	0.6	2.5	1
9	1400	0.8	2.7	0

Table 4 Table for N_2

Experiment number	Laser power (W)	Gas pressure (bar)	Cutting speed (m/min)	Focal position (mm)
1.	3000	8	1900	0
2.	3000	9	2000	−1
3.	3000	10	2100	1
4.	3500	8	2000	1
5.	3500	9	2100	0
6.	3500	10	1900	−1
7.	4000	8	2100	−1
8.	4000	9	1900	1
9.	4000	10	2000	0

The input parameter/dependent parameter and output/independent parameter are to be optimized using nine different experiments, which have been carried out as shown in Table 4. This parameter is taken by using nitrogen as an inert gas. However, we have four variables and three levels. Table 4 shows the table for nitrogen.

Based on Taguchi, we had conducted nine experiments with four input parameters like gas pressure, cutting speed, laser power and focal point. Tables 3 and 4 show the design of experiments for nitrogen and oxygen, respectively. We had calculated material removal rate and surface roughness. Surface roughness is found using non-contact-type Talysurf. The calculated material removal rate and surface roughness on titanium alloy (Ti 3Al-2.5V) using oxygen and nitrogen gases are shown in Table 5. With these response parameters like surface roughness and material removal rate, the optimal setting of predominant process parameter is found by using Grey-Taguchi analysis (Fig. 1).

Table 5 Table for MRR and SR

Experiment no	Material removal rate (m^3/min)		Surface roughness (μm)	
	Oxygen	Nitrogen	Oxygen	Nitrogen
1.	208.2	310.1	7.78	6.83
2.	210.4	321.56	7.27	4.36
3.	148.39	257.16	2.43	1.32
4.	213.37	324.6	6.71	4.81
5.	229.68	347.35	2.78	1.14
6.	269.19	398.44	4.83	2.05
7.	269.41	399.1	6.87	3.43
8.	287.49	414.18	6.17	2.65
9.	188.09	287.97	11.6	8.06

Fig. 1 Work piece specimen

3 Results and Discussion

3.1 Taguchi Optimization

Dr. Taguchi from Japan has introduced a method based on orthogonal array, which gives us much lesser variation to obtain optimum setting of the control parameter that is given as a design in Taguchi method.

3.2 Grey Relation Analysis

It works on using a specific concept of information similar to that of binary algebra. If the information is present and it is perfect, then it is regarded as white. Similarly, if no information is present, then it is portrayed as black. However, perfectly black or white is regarded as an idealized case, and in reality, it always lies between black and white.

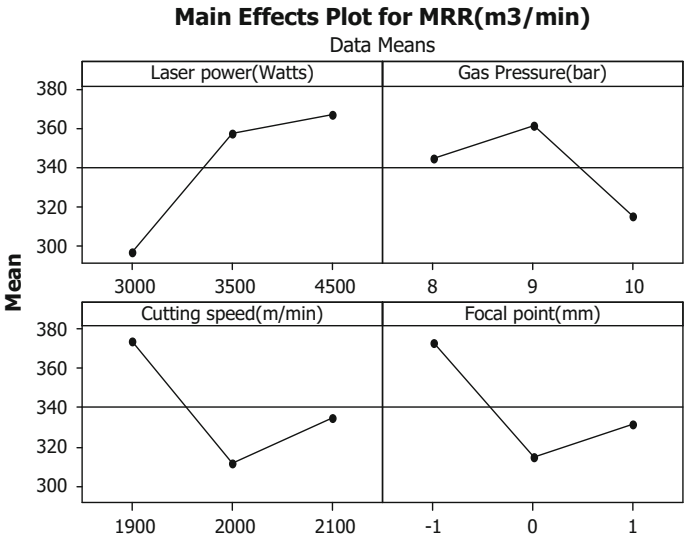

Fig. 2 Main effect plots for MRR of N_2

3.3 Steps Involved in Grey-Relational Analysis

Step-1 Transform the given information into S/N curve, otherwise called as shear strength vs number of cycles into Y_{nj} using suitable equation depending upon quality characteristics.

Step-2 After obtaining the *S/N* ratio, next task is to normalize the given date evenly and scale it to acceptable range for further analysis.

Step-3 Final step is to calculate the grey coefficient for the given normalized *S/N* ratios.

3.4 Grey-Relational Optimization

Grey relation method is the technique used for solving interrelationships among the multiple responses. This analysis follows the following steps:

Step-1 After transferring the responses into *S/N* ratio Y_{nj} using the suitable equations depending upon the quality characteristics (Table 6)

$$S/N \text{ RATIO OF MRR } = -10 * \log(1/X) \sum \left(1/Y_{nj}^2\right)$$

$$S/N \text{ RATIO OF SR} = -10 * \log(1/x) \sum Y_{nj}^2$$

Table 6 Values of *S/N* ratio to normalized *S/N* ratio

Ex No.	Material removal rate (mm^3/min)				Surface roughness (μm)			
	S/N ratio of O_2	*S/N* ratio of N	Normalized *S/N* ratio of O_2	Normalized *S/N* ratio of N	*S/N* ratio of O_2	*S/N* ratio of N	Normalized *S/N* ratio of O_2	Normalized *S/N* ratio of N
1.	46.36	49.83	0.51	0.42	−17.81	−16.68	0.71	0.90
2.	46.46	50.14	0.52	0.50	−17.23	−12.78	0.67	0.66
3.	43.42	48.20	0	0	−7.71	−2.41	0	0
4.	6.58	50.22	0.54	0.52	−16.53	−13.64	0.62	0.71
5.	47.22	50.81	0.66	0.68	−8.88	−3.40	0.08	0.06
6.	48.60	52.02	0.90	0.99	−13.67	−6.23	0.42	0.24
7.	48.60	52.03	0.90	1	−16.73	−10.70	0.63	0.52
8.	49.17	52.34	1	1	−10.02	−8.46	0.16	0.38
9.	45.48	49.18	0.35	0.28	−21.28	−18.12	0.27	1

Table 7 Values of grey relation rank and grade

Ex. no	Grey-relational coefficient				Grey-relational grade		Rank	
	MRR		SR					
	O_2	N_2	O_2	N_2	O_2	N_2	O_2	N_2
1.	0.48	0.60	0.33	0.51	0.59	0.5	5	2
2.	1	0.33	1	0.33	0.33	0.33	6	4
3.	0.46	0.56	0.38	0.52	0.63	0.51	4	3
4.	0.34	0.35	0.91	0.56	0.34	0.60	7	1
5.	0.1	0.46	0.58	0.83	0.39	0.98	8	5
6.	0.1	0.57	0.37	0.83	0.51	1	2	6
7.	0	0.37	0.84	1	0.44	1	3	8
8.	0.65	0.40	0.73	0.43	1	0.28	1	9
9.	0.1	0.50	0.53	0.82	0.40	0.50	9	7

Step-2 To normalize the *S*/*N* ratio to the acceptable range and to distribute the data evenly using the following equation

$$\text{NORMALIZED } S/N \text{ OF MRR } Z_n = \left(Y_{\text{nj}} - \min Y_{\text{nj}}\right)/\left(\max Y_{\text{nj}} - \min Y_{\text{nj}}\right)$$
$$\text{NORMALIZED } S/N \text{ OF SR } Z_{\text{nj}} = \left(\max Y_{\text{nj}} - Y_{\text{nj}}\right)/\left(\max Y_{\text{nj}} - \min Y_{\text{nj}}\right)$$

where Z_{nj} is the normalized value of nth trial for nth dependent response.

Step-3 To calculate the grey coefficient (GC) for the normalized *S*/*N* ratio values as per the following equation.

$$\text{GC}_{\text{nj}} = (\Psi\min + \delta\Psi\max)/(\Psi_{\text{nj}} + \delta\Psi\max),$$

where GC is the grey coefficient for the *n*th trial of the dependent response, *d* is called the quality loss, and Ψ is the distinctive coefficient which has a range from 0 to 1 (Table 7).

The highest max–min value in the Tables 8 and 9 shows that high stand-off distance as the most influencing parameter on determining the response characteristics.

3.5 Effects of Process Parameters on MRR

The effect of gas pressure on MRR was tested in range from 0.6 to 1.0 bar. In this range, it was found that when the gas pressure increased, the MRR was almost of a fixed value. The tests were repeated at two different gases. Therefore, it is concluded that gas pressure has no effect on MRR in the test range. The test result of the effect of jet pressure on the MRR at different gasses. A number of experiments

Table 8 Average grey-relational grade for each input parameter of O_2

Control factor	Average grey-relational grade			Max–min
	Level 1	Level 2	Level 3	
Laser power (w)	0.486	0.548	0.611	0.123
Gas pressure (bar)	0.6038	0.564	0.477	0.126
Cutting speed (m/min)	0.6308	0.517	0.498	0.132
Focal point (mm)	0.4784	0.551	0.523	0.072

Table 9 Average grey-relational grade for each input parameter of N_2

Control factor	Average grey-relational grade			Max–min
	Level 1	Level 2	Level 3	
Laser power (W)	0.486	0.548	0.599	0.11
Gas pressure (bar)	0.6038	0.564	0.403	0.200
Cutting speed (m/min)	0.6306	0.5033	0.498	0.1326

were carried out to find the relations between the laser power and MRR [7]. During these tests, the laser power is varied from 1200 to 4000 W and the tests were repeated for cutting speed of 2.5–2.9 m/mm. It shows that MRR decreases with the increase of laser power. A number of experiments were carried to find the relations between the cutting speed and MRR. During these tests, the cutting speed varies from 2.5 to 2.9 m/mm. It shows that MRR increases with the increase of cutting speed. Main effect plots for MRR of oxygen are shown in Fig. 3. The MRR values were tested at four different focal points. The tests were repeated at three different laser powers. The tests show that the MRR values are nearly constant at different focal point. Therefore, it is concluded that the focal point distance has no effect on MRR value (Fig. 2).

3.6 Effect of Process Parameter on SR

The effect of gas pressure on surface roughness Ra parameter was tested under ranges of pressure 0.6–1 bar. In this range, it was found that when the gas pressure increased, the roughness Ra parameter was almost of a fixed value. The test was repeated using two inert gasses. Therefore, it is concluded that gas pressure had no effect on surface roughness Ra parameter in the test range. The effect of gas pressure on the surface roughness Ra parameter at different gasses. The surface roughness Ra parameter values were measured at different cutting speed that range from 2.1 to 2.5 m/min and the two different gasses [8]. As the cutting speed increases, the surface roughness decreases. The relation trend is of power function with medium regression ratio. Main effect plots for SR of nitrogen gas are as shown

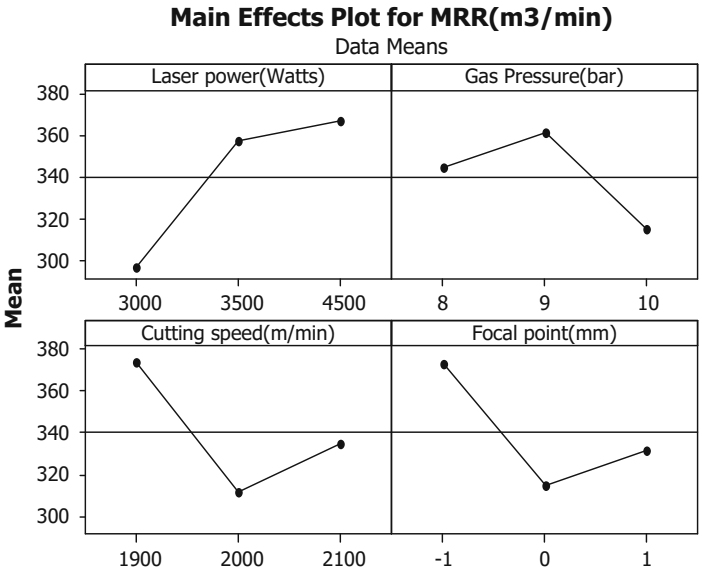

Fig. 3 Main effect plots for MRR of O_2

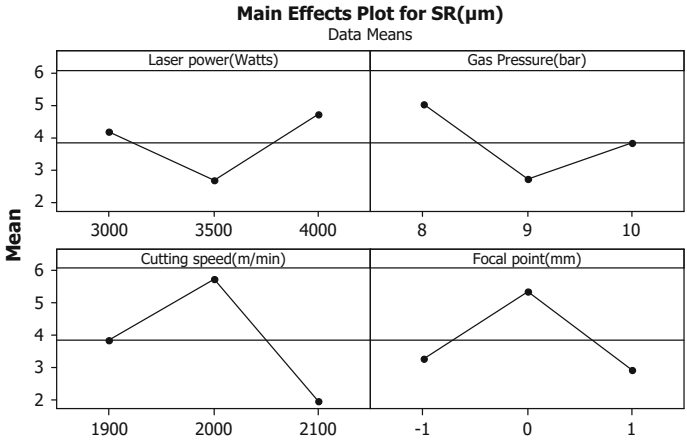

Fig. 4 Main effect plot for SR of N_2

in Fig. 4. The surface roughness Ra parameter values were tested at a range of laser power from 1200 to 4000 W [9]. The tests were repeated at two different cutting speeds. The surface roughness Ra values are nearly constant at different gasses. The higher the cutting speed yields, the lower the surface roughness. Main effect plot for SR of oxygen is shown in Fig. 5 [10].

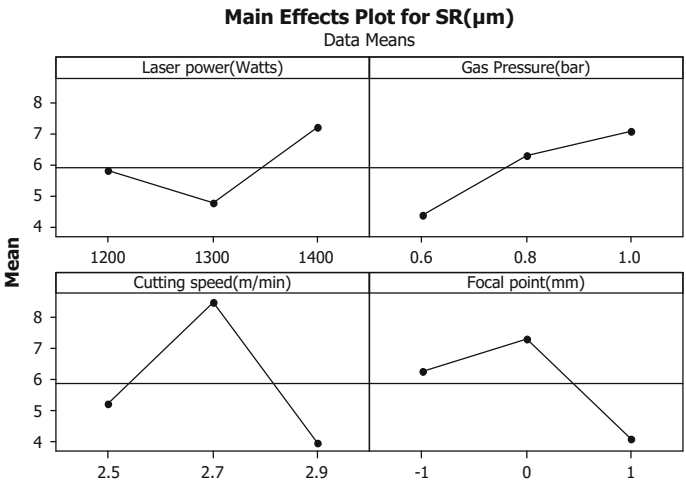

Fig. 5 Main effect plot for SR of O_2

1. Gas pressure—10 bar, cutting speed—1.9 m/min, laser power—4000 W, focal point—1 mm.

The better surface roughness of nitrogen gas because of low laser power and high focal point and the Ra value for better surface roughness for nitrogen is 4.2 µm. The parameters are shown in Fig. 6 [11].

2. Gas pressure—10 bar, cutting Speed—2.1 m/min, laser power—3000 W, focal point—1 mm.

The poor surface finishes value of oxygen gas because of gas pressure, cutting speed, laser power and focal point. The Ra value for poor surface roughness for nitrogen is 8.4 µm. Graphs are shown in Fig. 7.

3. Gas pressure—10 bar, cutting speed—2.1 m/min, laser power—1400 watts, focal point—1 mm.

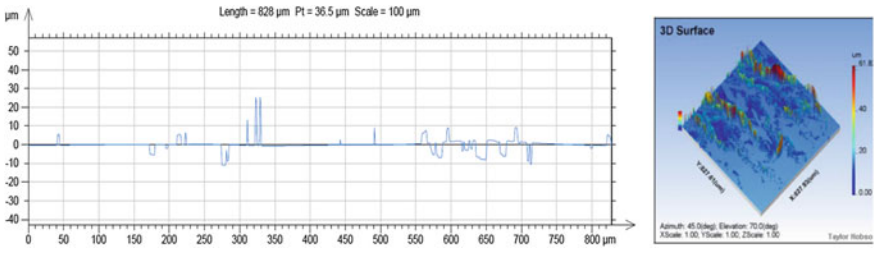

Fig. 6 2D and 3D graphs for better surface roughness for N_2

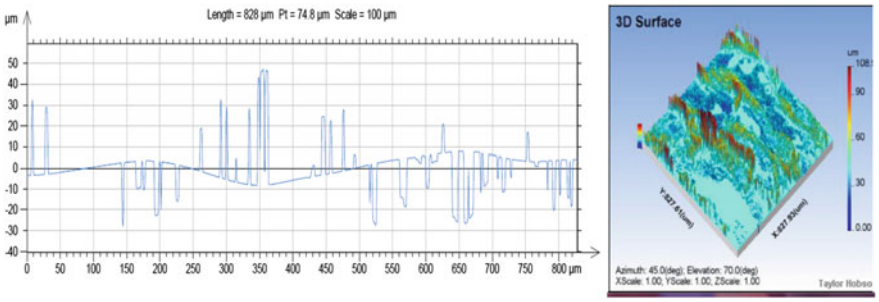

Fig. 7 2D and 3D graphs for poor surface roughness for N_2

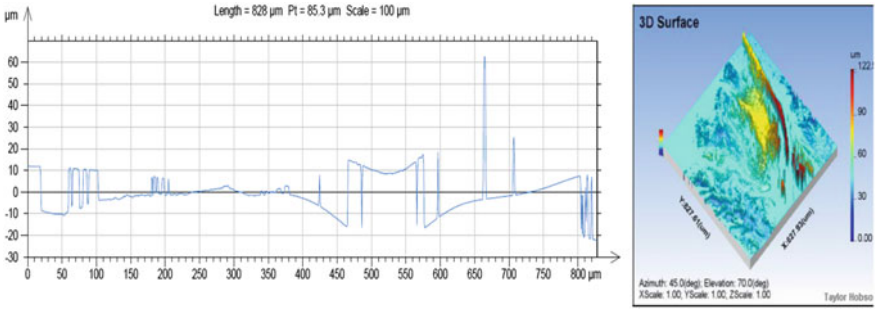

Fig. 8 2D and 3D graphs for better surface roughness for O_2

The better surface roughness of Oxygen gas because of low Laser power and High focal point. The Ra value for better surface roughness for oxygen is 7.2 µm. Graphs are shown in Fig. 8.

4. Gas pressure—10 bar, cutting speed—2.1 m/min, laser power—1200 W and focal point—1 mm.

The poor surface roughness of Oxygen gas because of low Laser power and High focal point [12]. The Ra value for poor surface roughness for oxygen is 11.5 µm. Graphs are shown in Fig. 9. The optimized graph of both oxygen and nitrogen is shown in 2D and 3D in Fig. 9 [13].

5. Gas pressure—10 bar, cutting speed—1.9 m/min, laser power—1400 W, focal point—1 mm.

The comparison of oxygen and nitrogen gasses give influence of low surface roughness. Graphs are shown in Figs. 10, 11 and 12.

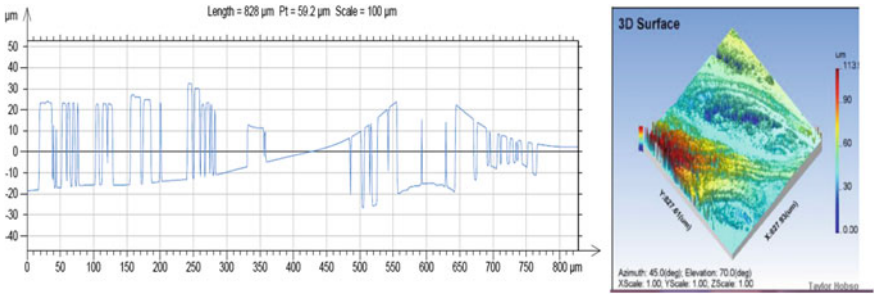

Fig. 9 2D and 3D graphs for poor surface roughness for O_2

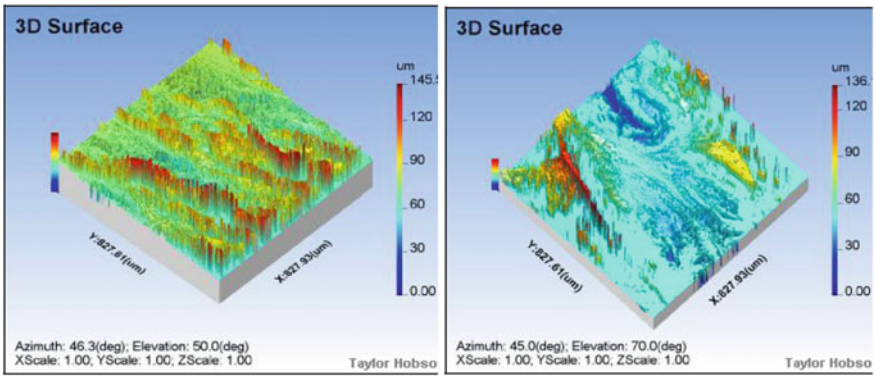

Fig. 10 3D graph for optimized value of O_2 and N_2

Fig. 11 Structure for N_2

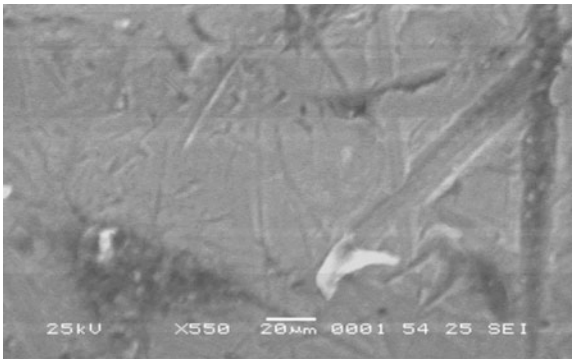

Fig. 12 Structure for O_2

3.7 SEM Analysis

Under scanning electron microscope (SEM), the specimen of the work piece is viewed and the image is obtained as shown below. The parameters are selected for the following parameters, gas pressure—10 bar, laser power 4000 W, type of cut—rough cut and cutting speed—2.1 m/min, magnification ratio of 100 µm. The below Fig. 13 shows a structure for nitrogen, and the Fig. 14 shows a structure for oxygen [14].

The below shown figure shows scanning electron microscope (SEM) image for poor and better work piece for heat-affected zone. The parameters are selected for the following parameters for better: gas pressure—10 bar, cutting speed—2.1 m/mm, laser power—4000 W, type of cut—rough cut, magnification ratio of 150 µm. The below Fig. 13 shows a better image for nitrogen, and the Fig. 14 shows s poor image for oxygen.

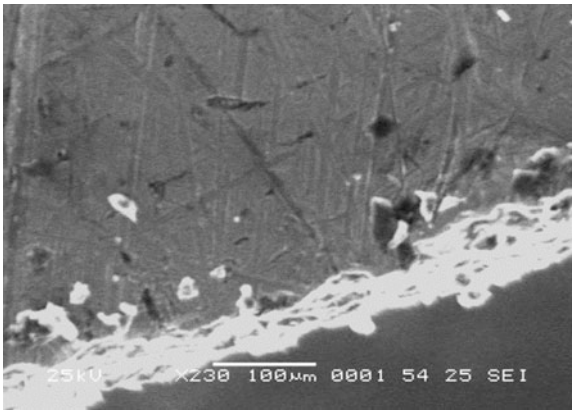

Fig. 13 Better image for N_2

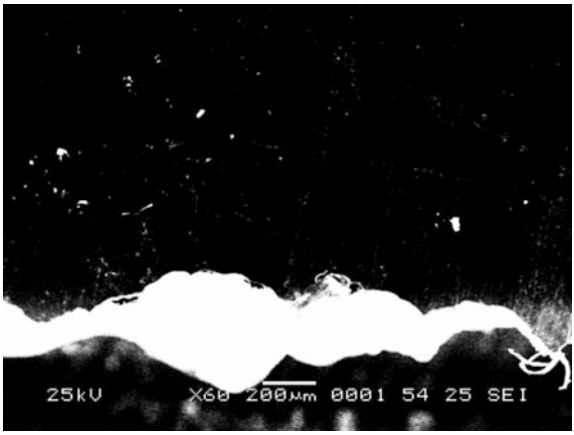

Fig. 14 Better image for O_2

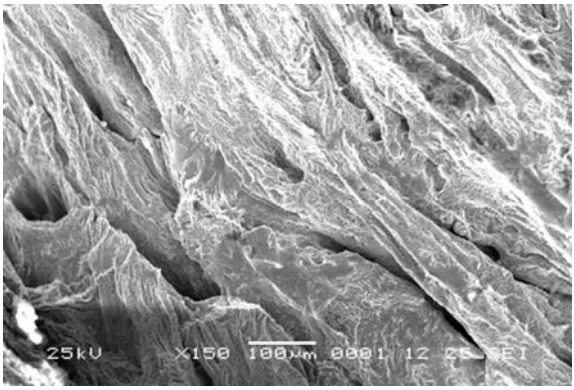

Fig. 15 Machined surface of N_2

The below shown figure shows scanning electron microscope (SEM) for poor and better work piece for machined surface. These parameters are selected for the following parameters for better: gas pressure—10 bar, cutting speed—2.1 m/min, laser power—3000 W, type of cut—rough cut, magnifications ratio of 150 µm. The optimized values are obtained the experiment in which the grey-relational grade is ranked 1 of 9 experiments. The optimized values for various machining parameters are Material removal rate [15] is 45.6(g/min) and Surface roughness is 5.6 (µm). The above Fig. 15 shows a machined surface of nitrogen, and the Fig. 16 shows a machined surface of oxygen.

3.8 Confirmation Test

After obtaining the optimized values for material removal rate (MRR), surface roughness test had been carried out to verify the integrity of the results obtained.

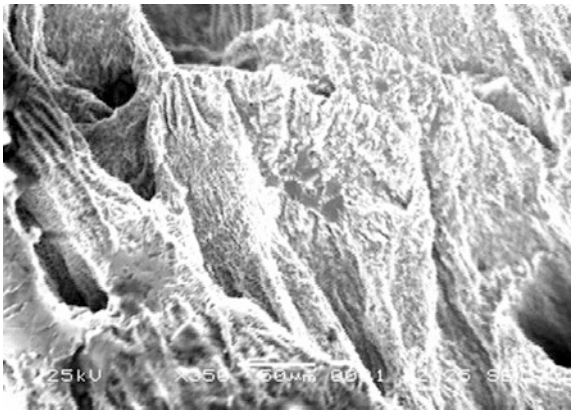

Fig. 16 Machined surface of O_2

Finally, the satisfactory values are: MRR is 45.6 (g/min) and surface roughness is 5.6 (μm). As per 95% of confidence limit, the errors obtained for each of the response parameters are MRR: 4% error and surface roughness: 3.5% error. In this paper, titanium alloy (TiA3lV) was machined using one of the non-traditional machining processes called CO_2 laser beam machining. This alloy was chosen based on its prime application as a washer used in high-pressure turbine. The input parameters—laser power, gas pressure, cutting speed and focal point—were suitable varied to get the optimum values of response parameters like metal removal rate, surface roughness and heat-affected zone. The machining parameters were optimized using Grey-Taguchi approach, and it was confirmed by conducting a confirmation test. The graph which was generated using Minitab 17 software clearly represents of each input parameters over the response parameter. As per 95% of confidence limit, the error obtained for each of the response parameters are material removal rate is 4.67% error and Surface roughness is 3.25%. Through this experiment, we have learnt that Grey-Taguchi methodology can be effectively used to produce the optimum levels of machining parameters involved in CO_2 laser beam machining process.

4 Conclusion

In this present work, titanium alloy (Ti3Al2.5V) is machined using CO_2 laser beam machining. Titanium alloy is selected based on its applications in aerospace industries and high-pressure turbines, etc. The predominant input parameters like laser power, gas pressure, cutting speed and focal point were suitably varied to get optimum values of response parameters like material removal rate, surface roughness. These machining parameters are optimized using Taguchi-Grey analysis. The most suitable and optimal combination of the process parameter for getting better response parameter is found. The optimized satisfactory value of material removal

rate is 45.56 m^3/min and surface roughness is 3.5 μm under the condition of 4000 bar gas pressure, 2100 m/min cutting speed, type of rough cut and 1 mm of focal point. The most influencing factors for getting better material removal rate are cutting speed and pressure. The most influencing factors for getting better surface roughness are focal point and type of cut. It is found that SR and MRR are increased by 35 and 42%, respectively, while using nitrogen in place of oxygen in CO_2 laser beam machine. The confirmation test is carried out to check the integrity of the result obtained, and error percentage is found to be 4.67 and 3.25% for material removal rate and surface roughness, respectively.

References

1. Chen, K., Yaoh, Y.L., Modi, V.: Gas dynamic effects on laser cutting quality. J. Manuf. Process. **3**(No1), 38–49 (2001)
2. Chen, S.L.: analysis and modeling of reactive three-dimensional high-power CO2 laser cutting. Proc. I MECH E Part B J. Eng. Manuf. **212**(2), 113–128 (1998)
3. Asano, H., Suzuki, J., Kawakami, E.: Selection of parameters on laser cutting mild steel plates taking account of some manufacturing purposes. In: Fourth International symposium on laser precision microfabrication. Proceedings of SPIE, vol. 5063, pp. 418–425 (2003)
4. Di Pietro, P., Yaoh, Y.L.: An investigation into characterizing and optimizing laser cutting quality—a review. Int. J. Mach. Tools Manuf. **34**(2), 225–243 (1994)
5. Espinal, D., Kat, A.: Thermochemical modeling of oxygen-assisted laser cutting. J. Laser Appl. **12**(1), 16–22 (2000)
6. Mas,C., Fabbro, R.: Steady-state laser cutting modeling. J. Laser Appl. **15**(3), 145–152 (2003)
7. Chen, K., Lawrence Yaoh, Y., Modi, Vijay: Numerical simulation of oxidation effects in the laser cutting process. Int. J. Adv. Manuf. Technol. **15**(11), 835–842 (2004)
8. Lu, C.: Study on prediction of surface quality in machining process. J. Mater. Process. Technol. **205**(1–3), 439–450 (2008)
9. Chen, K., Yao, Y.L., Modi, V.: Gas jet-workpiece interactions in laser machining. J. Manuf. Sci. Eng. **122**, 429–438 (2000)
10. Jimin, C., Jianhua, Y., Shuai, Z., Tiechuan, Z., Dixin, G.: Int. J. Adv. Manuf. Technol. **33**(5–6), 469–473 (2007)
11. Ermolaev, G.V., et al.: Mathematical modelling of striation formation in oxygen laser cutting of mild steel. J. Phys. D Appl. Phys. **39**, 4236–4244 (2006)
12. Chen, S.-L.: Thermal modelling of cutting front edge dynamic behaviour in high-power reactive CO2 laser cutting. Proc. I MECH E Part B J. Eng. Manuf. **212**(7), 555–570 (1998)
13. Farooq, K., Kar, A.: Removal of laser-melted material with an assist gas. J. Appl. Phys. **83** (12), 7467–7473 (1998)
14. Gabzdyl, J.T., Morgan, D.A.: Assist gases for laser cutting of steels. In: ICALEO, pp. 443–447 (1992)
15. Yousef, B., Knopf, G.K., Bordatchev, E.V., Nikumb, S.K.: Neural network modeling and analysis of material removal process during laser machining. Int. J. Adv. Manuf. Technol. **22** (1–2) (2003)